Molecular Crystals and Liquid Crystals
Publication details, including instructions for authors and subscription information:
http://www.tandfonline.com/loi/gmcl16

# Dielectric, Electro-Optical and Phase-Change Properties of Liquid Crystal Guest-Host Displays

M. Schadt [a] & P. Gerber [a]
[a] Central Research Units, Basel, F. Hoffman. La Roche & Co., Ltd. CH., 4002, Switzerland.
Version of record first published: 20 Apr 2011.

To cite this article: M. Schadt & P. Gerber (1981): Dielectric, Electro-Optical and Phase-Change Properties of Liquid Crystal Guest-Host Displays, Molecular Crystals and Liquid Crystals, 65:3-4, 241-264

To link to this article: http://dx.doi.org/10.1080/00268948108082137

*Mol. Cryst. Liq. Cryst.*, 1981, Vol. 65, pp. 241–264
0026-8941/81/6504-0241$06.50/0




# Dielectric, Electro-Optical and Phase-Change Properties of Liquid Crystal Guest-Host Displays

M. SCHADT and P. GERBER

*Central Research Units, F. Hoffman . La Roche & Co., Ltd., CH . 4002 Basel, Switzerland.*

*(Received June 5, 1980)*

We present novel measurements and correlations between the electric field-induced change of capacitance, optical appearance and material parameters of nematic as well as cholesteric guest-host layers. New guest-host mixtures comprising various dichroic dyes with transition moments parallel (L-dyes) and perpendicular (T-dyes) to the nematic director exhibiting large dichroic ratios and UV-stability were used. The material parameters determining the capacitive as well as the electro-optical characteristics, including all elastic constants, were measured. Good agreement was found between measured and numerically calculated characteristics when using the experimentally determined material parameters in the formalism derived to calculate the transmission characteristics of homogeneous nematic guest-host displays. It is shown that the field-induced dielectric changes occurring in cholesteric guest-host layers with parallel and homeotropic wall alignment respectively differ considerably from their electro-optical characteristics in reflective displays. The phase-change calculations used so far are shown to be inadequate to explain the experimental findings.

## INTRODUCTION

Most investigations into liquid crystal display phenomena have concentrated on the electro-optical properties of the devices and on those of the effects on which they are based. Because of the complexity of most quantitative electro-optical calculations as well as the experimental difficulties faced when attempting to determine some crucial liquid crystal material properties such as the elastic constants, only a few studies have been reported in which complete sets of experimentally determined liquid crystal parameters were related to their actual electro-optical behaviour in displays. Even fewer attempts have been made to measure and relate electric field-induced dielectric changes with electro-optical properties of liquid crystal layers.

To our knowledge there has been only one attempt so far in which the field-induced dielectric changes occurring in guest-host layers were correlated with their electro-optical characteristics and the properties of the liquid crystal material.[1] In the present study we continue our previous work.[1] Apart from homogeneously (parallel) aligned nematic guest-host displays we investigate cholesteric-nematic phase change displays[2] with homogeneous and homeotropic boundaries respectively. It will be shown that the electro-optical characteristics of reflective phase-change displays differ strongly from the field-induced capacitance changes; the differences being due to the liquid crystal- and dichroic-dye properties, as well as to the mechanisms governing the phase transitions. The elastic and dielectric constants of new high contrast and UV-stable nematic guest-host mixtures are determined and related to the voltage dependence of numerically calculated as well as measured transmission characteristics. Homogeneous nematic[3] as well as colour changing displays of the L/T-type[1] are studied.

## MEASURING METHODS

The schematic in Figure 1 shows the measuring principle used to determine the capacitance changes $\Delta C(V)/\Delta C_{max}$ occurring in an initially parallel

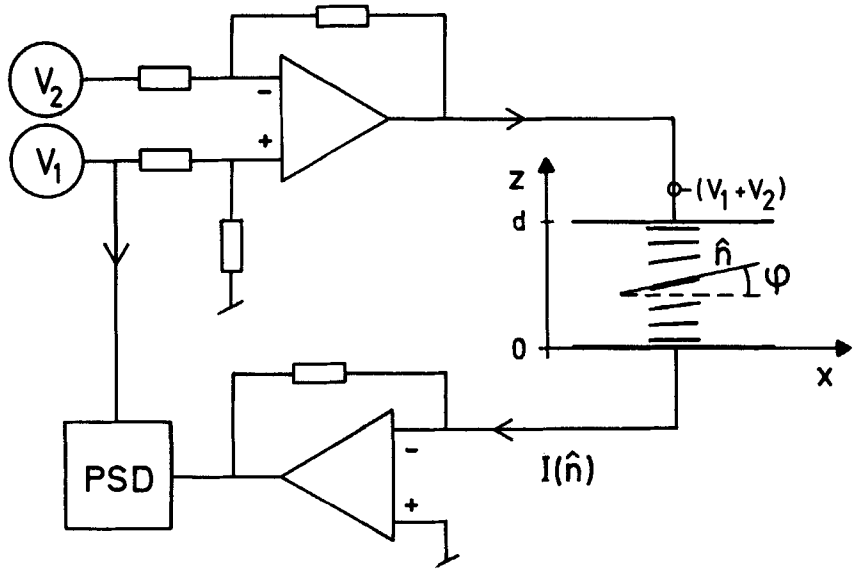


FIGURE 1 Schematic of the apparatus used to measure the voltage-induced capacitance changes of liquid crystal layers. As an example a homogeneously aligned nematic cell is shown where $\phi$ is the angle between the nematic director $\hat{n}(V, z)$ and the $x$-direction.

aligned liquid crystal layer of thickness $d$ upon application of an electric field; $(\Delta C(V) = [C(V) - C(V = 0)]$, $\Delta C_{max} = [C(V \to \infty) - C(V = 0)]$. The voltage $V_1 = 20$ mV and the swept voltage $V_2 = 0$–50 volts with the respective frequencies $f_1 \neq f_2$ are the capacitance-detecting and the aligning voltage. The total deformation of the positive dielectric layer for voltages $V_2 > V_t$, $V_t$ = threshold voltage, induces a change of the capacitive current $I(\hat{n}, V_1(f_1)]$ which is measured by the phase sensitive detector PSD. The angle $\phi$ denotes the deflection of the nematic director $\hat{n}(z)$ from the $x$-direction (Figure 1). To perform the field-induced measurements in a quasi stationary state the amplitude of the aligning voltage can be swept as slowly as 1 volt/2 hours. $V_2(\text{max}) = 50$ volts was found to be sufficiently large to induce complete homeotropic alignment in initially homogeneously aligned 20 $\mu$m cells. The dielectric constants $\varepsilon_\perp(V_2 = 0$ volts) and $\varepsilon_\parallel(V_2 = 50$ volts) determined with the apparatus shown in Figure 1 agree within 0.5% with those from measurements made in magnetic-field aligned samples using 1 mm electrode spacing. A detailed description of the measuring principle similar to the one in Figure 1 was published earlier.[4]

The spectra, the voltage dependence of the optical transmission of guest-host displays at a given wavelength, the dichroic ratios and order parameters $S$ of dichroic dyes dissolved in nematic hosts were measured with a modified dual beam model 200 Perkin–Elmer photospectrometer incorporating a Glenn–Thompson polarizing prism. The influence of the nematic host on the measurements was eliminated by mounting identical homogeneously aligned cells in both reference and sample beam. The reference cell was filled with the nematic host only, whereas the sample cell contained the guest-host mixture. The same instrument was used to determine the spacing of the empty display by measuring the wavelength dependence of the transmission interference pattern.

The electro-optical transmission and reflection measurements with white light were made with a Leitz Orthoplan Pol microscope. A diffuse reflecting barium sulfate coating was painted on the back plate of the cell when measuring in reflection. Homogeneous wall alignment with bias tilt angles $<0.3°$ was achieved by angular evaporation of $SiO_2$; whereas the glass plates were dipped in an 0.3% lethitin/aethanol solution to obtain homeotropic wall alignment. All experiments were performed at 22°C.

## LC-MATERIALS AND DYES

Unless otherwise stated all LC-materials and dyes used are from F. Hoffmann–La Roche. The positive dielectric mixtures RO–TN–605 and RO–TN–655 were used as hosts for the experiments. Both exhibit large meso-

morphic ranges, high nematic-isotropic transition temperatures $T_c$ and—despite their large positive dielectric anisotropy $\Delta\varepsilon = (\varepsilon_{\parallel} - \varepsilon_{\perp})$—a low bulk viscosity $\eta$. The mixtures contain essentially liquid crystal components belonging to the classes of aromatic and hydrogenated esters, pyrimidines and to the recently described hydrogenated terpyrimidines.[5] Besides, RO-TN-655 contains about 40% phenyldioxanes

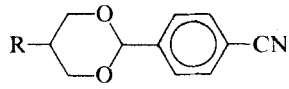

a new LC-class with low optical anisotropy combined with a relatively large positive dielectric anisotropy. Both mixtures induce a high degree of order in dichroic dyes. The UV-stability of dyes in RO-TN-605 is exceptionally good. Table I shows some data of the two hosts.

TABLE I

Mesomorphic, viscous, dielectric and optical material properties of nematic host mixtures. Measurements made at 22°C

| LC | $T_m$ [°C] | $T_c$ [°C] | $\eta$ [cp] | $\varepsilon_{\perp}$ | $\Delta\varepsilon$ | $n_0$ | $\Delta n$ |
|---|---|---|---|---|---|---|---|
| RO-TN-605 | $< -20$ | 96 | 49.4 | 5.28 | +13.08 | 1.500 | 0.172 |
| RO-TN-655 | $< -20$ | 100 | 57.6 | 6.22 | +15.75 | 1.491 | 0.142 |
| RO-TN-605 + 5% T-dye | — | 103 | — | 5.06 | +13.32 | 1.500 | 0.174 |

Two principally different types of dichroic dyes were used in the experiments, namely T-dyes[1] with transition moments perpendicular to their long molecular axis, i.e. perpendicular $\hat{n}$ and L-dyes with transition moments parallel $\hat{n}$. A liquid crystalline tetrazine dye T served as a T-dye.[1,6] Whereas a new blue anthraquinone L-dye B with improved order parameter and

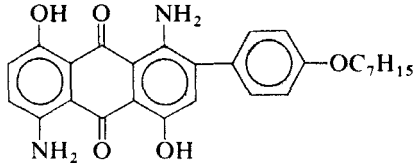

solubility was used. Besides, a new red and yellow dye denominated R and Y with UV-stability, solubility (>2%) and degree of order comparable to that of the blue dye B were used.

Figure 2 shows the absorption spectra of dyes B and T in the homogeneously aligned host RO-TN-605. Both spectra were recorded with light

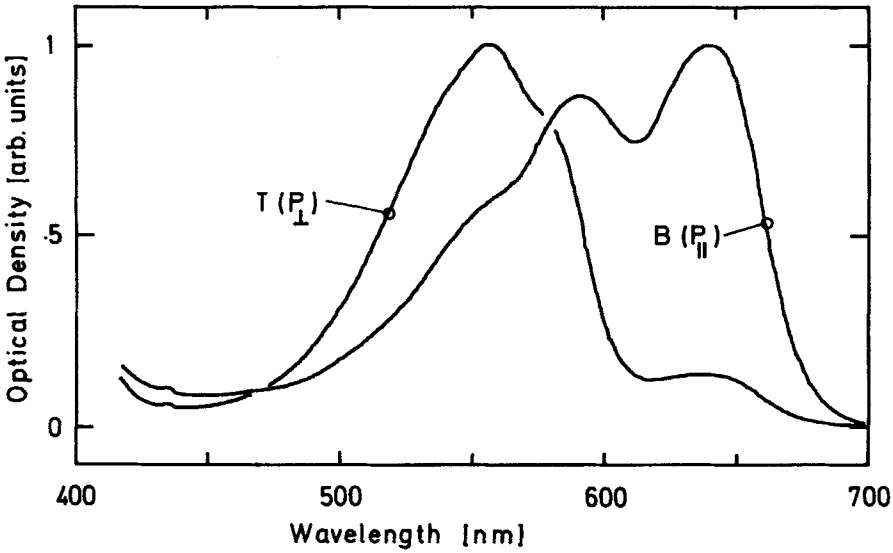


FIGURE 2 Absorption spectra of the red T-dye and the blue L-dye B recorded in parallel aligned RO-TN-605 with light polarized perpendicular ($P_\perp$) and parallel ($P_\parallel$) to the nematic director respectively.

polarized along the respective directions of maximum dye absorption; i.e. $P \perp \hat{n}$ for the T-dye and $P \parallel \hat{n}$ for the L-dye, $P$ being the direction of polarization. Because of the weak $n - \pi^*$ transition, causing the red colour of tetrazines, a rather large T-dye concentration of 5% was used to obtain sufficiently strong extinction in 20 $\mu$m layers. This concentration was $\sim 10$ times larger than that used for dyes B, R and Y. At such a large guest concentration the material parameters of the host do not necessarily remain unchanged. We therefore measured the dielectric and elastic constants, determining the static electro-optical properties of guest-host displays of mixture RO-TN-605 incorporating 5% T-dyes separately.

A high contrast, black-white guest-host mixture denominated B11 was made by combining the three L-dyes B, R and Y in RO-TN-605. Figure 3 shows the individual spectra of the three dyes recorded with polarized light $P \parallel \hat{n}(P_\parallel)$ and $P \perp \hat{n}(P_\perp)$. From the measurements in Figure 3 follow dichroic ratios $r = \alpha_\parallel/\alpha_\perp > 8.8$ for B11 over the whole visible range.

Table II shows measurements of the individual dye order parameters $S$ determined in RO-TN-605 using equations derived earlier.[1] Also depicted in Table II are the isotropic molar extinction coefficients $\alpha_0$ measured

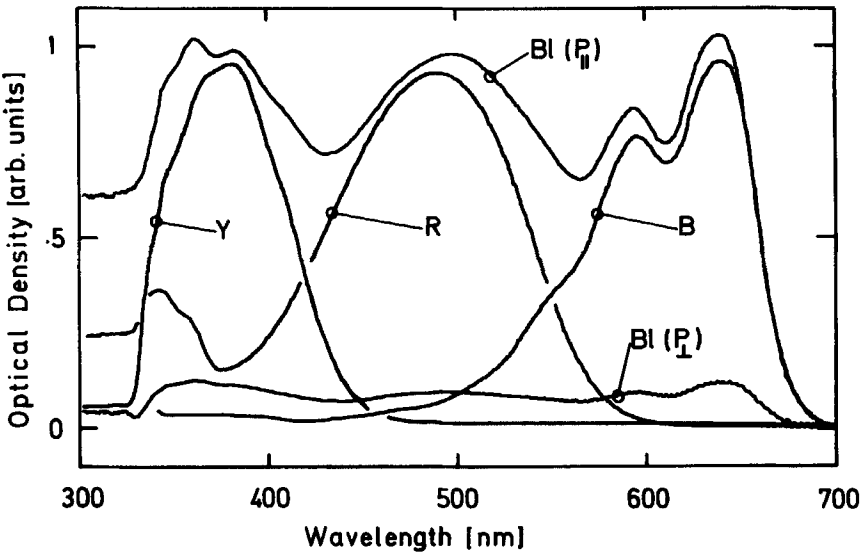


FIGURE 3 Absorption spectra of the yellow (Y), red (R) and blue (B) L-dye components used in Bl 1. The spectra Bl are those of the black-white mixture recorded with light polarized parallel ($P_\parallel$) and perpendicular ($P_\perp$) to $\hat{n}$ respectively.

TABLE II

Wavelength $\lambda_{max}$ of maximum isotropic extinction $\alpha_0$; order parameter S and lifetime $t_{70}$ measured in RO-TN-605 at 22°C of L- and T-dichroic dyes B, R, Y and T respectively

| Dye | $\lambda_{max}$ [nm] | $\alpha_0 \times 10^4$ | S | $t_{70}$ [hours] |
|---|---|---|---|---|
| B | 641 | 3.02 | 0.72 | > 700 |
| | 599 | 2.50 | | |
| R | 489 | 3.59 | 0.74 | 700 |
| Y | 381 | 2.39 | 0.72 | > 500 |
| T | 553 | 0.05 | 0.75 | — |

at the wavelength of maximum extinction $\lambda_{max}$, as well as the lifetimes $t_{70}$ of the dyes when exposed to intense white (UV) light in unprotected reflecting 10 $\mu$m displays. $t_{70}$ is the exposure time after which the display extinction diminishes to 70% of its initial value. The UV-tests were made by exposing the displays to a 1.1 kW Xenon lamp at a distance of 22 cm in a Hallau Sun-Test apparatus.

## HOMOGENEOUS NEMATIC GUEST-HOST DISPLAYS

### A Calculation of the transmission characteristics



It was shown earlier[1] that the electro-optical transmission of homogeneously aligned nematic guest-host displays containing L- or T-dyes can be described by analytical expressions for small angles of deformation. For voltages V exceeding the threshold voltage $V_t$ considerably the small angle approximation no longer holds and the electro-optical transmission characteristics have to be determined numerically. In the following we are going to derive approximate equations governing the electro-optical transmission of homogeneous L/T-guest-host displays for any electric field-induced deformation. The anisotropy of the refractive index will be neglected except for its absorptive part which is taken into account in leading order.

The total extinction $\alpha$ of a thin layer of L-dyes at the distance $z$ from the bottom electrode of a homogeneous nematic guest-host display (Figure 1) is given by[1]

$$\alpha[\phi(z)] = \alpha_{\parallel} - \Delta\alpha \sin^2 \phi = \alpha_i + 2\Delta\alpha/3 - \Delta\alpha \sin^2 \phi; \tag{1}$$

$\alpha_i$ = isotropic molar extinction coefficient, $\Delta\alpha = (\alpha_{\parallel} - \alpha_{\perp})$ = molar extinction anisotropy. From equation (1) follows for the optical density $D$ of the display

$$D \propto \frac{1}{d}\int_0^d \alpha[\phi(z)]\,dz = \alpha_i + \frac{2\Delta\alpha}{3} - \frac{\Delta\alpha}{d}\int_0^d \sin^2[\phi(z)]\,dz \tag{2}$$

$$= \alpha_i + \frac{2\Delta\alpha}{3} - \Delta\alpha\langle\sin^2\phi\rangle.$$

The mean value $\langle\sin^2\phi\rangle$ depends on the applied voltage; in particular

$$\langle\sin^2\phi\rangle = \begin{cases} 0, & V < V_t \\ \to 1, & V \to \infty \end{cases}$$

The threshold voltage is given by

$$V_t = \pi\left(\frac{k_{11}}{\varepsilon_o \Delta\varepsilon}\right)^{1/2}, \tag{3}$$

where $k_{11}$ is the splay elastic constant of the nematic host. Changing to the integration variable $\phi$ in

$$\langle\sin^2\phi\rangle = \frac{1}{d}\int_0^d \sin^2[\phi(z)]\,dz$$

one obtains

$$\langle \sin^2 \phi \rangle = \int_0^{\phi_m} \sin^2 \phi \left[ \frac{(1 + \kappa \sin^2 \phi)(1 + \gamma \sin^2 \phi)}{\sin^2 \phi_m - \sin^2 \phi} \right]^{1/2} d\phi \times \Big/ \int_0^{\phi_m} \left[ \frac{(1 + \kappa \sin^2 \phi)(1 + \gamma \sin^2 \phi)}{\sin^2 \phi_m - \sin^2 \phi} \right]^{1/2} d\phi, \quad (4)$$

where $\kappa = (k_{33}/k_{11} - 1)$, $k_{33}$ = bend elastic constant; $\gamma = (\Delta\varepsilon/\varepsilon_\perp)$. The angle $\phi$ of the nematic director $\hat{n}$ varies between $\phi(z = 0) = 0$ and $\phi(z = d/2) = \phi_m$ when moving from the bottom display boundary to the middle of the layer (Figure 1). The Jacobian

$$dz/d\phi = \left[ \frac{(1 + \kappa \sin^2 \phi)(1 + \gamma \sin^2 \phi)}{(\sin^2 \phi_m - \sin^2 \phi)} \right]^{1/2} \times \text{constant} \quad (5)$$

follows directly from the torque-balance equation of the electric-field-induced deformation of a nematic layer.[7] The maximum angle of deformation $\phi_m(z = d/2)$ is given by[7]

$$V/V_t = (1 + \gamma \sin^2 \phi_m)^{1/2} \times \int_0^{\phi_m} \left[ \frac{(1 + \kappa \sin^2 \phi)}{(1 + \gamma \sin^2 \phi)(\sin^2 \phi_m - \sin^2 \phi} \right]^{1/2} d\phi. \quad (6)$$

We determined the functional dependence

$$\langle \sin^2 \phi \rangle = f\left(\frac{V}{V_t}\right)$$

numerically by calculating the integrals in Eqs. (4) and (6) for different values of $\phi_m$ using the measured values for the elastic and the dielectric constants.

In the limit of small angles of deformation; i.e. $0 \leq (V - V_t)/V_t < 1$, Eq. (4) reduces to

$$\langle \sin^2 \phi \rangle = \left[ \frac{2}{(\gamma + \kappa + 1)} \right] \times \left[ \frac{(V - V_t)}{V_t} \right] + 0\left[ \frac{(V - V_t)}{V_t} \right]^2 + \cdots \quad (7)$$

Equation (7) is identical with the small angle approximation of the voltage dependence of the change of capacitance of a homogeneous nematic layer in the case where the alignment is purely field-induced;[4,7] i.e.

$$\frac{\Delta C(V)}{\Delta C_{\max}} = \left[ \frac{2}{(\gamma + \kappa + 1)} \right] \times \left[ \frac{(V - V_t)}{V_t} \right] + 0\left[ \frac{(V - V_t)}{V_t} \right]^2 + \cdots \quad (8)$$

### B Transmission characteristics and LC-parameters; results

The measurements of the capacitance changes $\Delta C(V)/\Delta C_{max}$ depicted in Figure 4 were made with $d = 20\ \mu m$ homogeneously aligned cells. The recordings *a* and *c* were made over the respective voltage ranges 0–50 and 0–10 volts using RO-TN-655. Graph *d* is a recording using RO-TN-605; whereas the dashed graph *b* shows $\Delta C(V)/\Delta C_{max}$ of a 90° twist cell containing RO-TN-655.

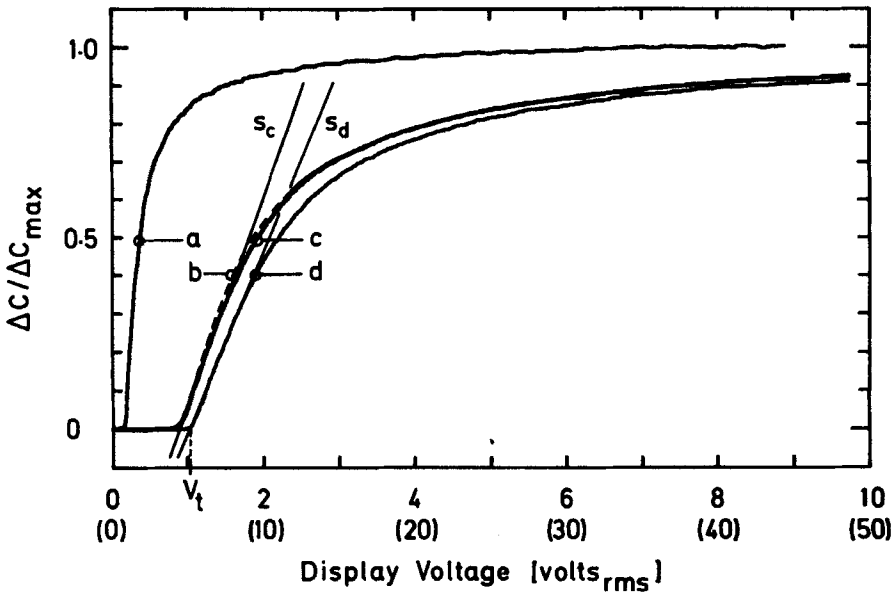


FIGURE 4 Measured capacitance versus voltage dependence of parallel (solid lines) and twisted nematic (dashed graph) cells. Graphs a, b and c were recorded using RO-TN-655, whereas graph d is a recording of RO-TN-605. The voltages in brackets refer to graph a only. $s_c$ and $s_d$ are the initial slopes of graphs c and d respectively.

The recordings in Figure 4 show that for both hosts complete homeotropic alignment, i.e. $\Delta C/\Delta C_{max} = 1$, occurs only at voltages $V > 35$ volts (graph *a*). Recording *c* of the stronger dielectric anisotropic RO-TN-655 exhibits a 10% lower threshold voltage $V_t$ and reaches 90% saturation of $\Delta C/\Delta C_{max}$ already at $V_{90} = 7.5$ volts compared with RO-TN-605 where $V_{90} = 8.5$ volts (graphs *d*). Besides an initially steeper slope, recording *b* of the twist cell coincides with the one of the homogeneous cell (graph *c*).

The measuring and evaluation methods to determine the splay ($k_{11}$), twist ($k_{22}$) and bend ($k_{33}$) elastic constants will be described in a separate article.[8] The results for RO-TN-605, RO-TN-655 and RO-TN-605

doped with 5% of the tetrazine T-dye are depicted in Table III. Using these data we have numerically calculated the voltage dependences $\Delta C(V)/\Delta C_{max}$ and found good agreement with the measurements shown in Figure 4. The determination of $k_{33}$ from the initial slopes $s_c$ and $s_d$ (Figure 4) using the small angle approximation (c.f. Eq. 8) yields the values in brackets (Table III). Comparing the data in Table III shows that the small angle approximation leads to values of $k_{33}$ that are up to 10% lower than those obtained from the numerical fit. The measurements also demonstrate that the large T-dye concentration in RO-TN-605 indeed changes the material properties of the host. $k_{11}$ and $k_{33}$ increase by $\sim 10\%$ upon doping (Table III) whereas $\Delta\varepsilon$ increases only by $\sim 2\%$ (Table I). The measuring accuracy for $k_{11}$ and $k_{22}$ is $\pm 3\%$, whereas that of $k_{33}$ is $\pm 4\%$.

TABLE III

Fréederickzs threshold voltage $V_t$ and elastic constants $k_{ii}$ measured at 22°C

| LC | $V_t$ [volts] | $k_{11}$ [$\times 10^{-12}$ N] | $k_{22}$ [$\times 10^{-12}$ N] | $k_{33}$ [$\times 10^{-12}$ N] |
|---|---|---|---|---|
| RO-TN 605 | 1.02 | 12.3 | 6.90 | 20.2 (19.3) |
| RO-TN-655 | 0.91 | 11.9 | 6.47 | 19.1 (17.4) |
| RO-TN-605 +5% T-dye | 1.05 | 13.1 | | 21.6 |

Figure 5 shows the voltage-induced extinction changes that were measured simultaneously with the capacitance changes (Figure 4). RO-TN-605 was used as a host for the recordings *a*, *b* and *T*, whereas RO-TN-655 was the host in measurement *c*. The experiments *a*, *b* and *c* were made with 0.4% of the guest L-dye B incorporated, where the T-dye guest concentration (graph T in Figure 5) was 5%. All measurements were made at the respective wavelengths of maximum extinction (Table II) using light polarized parallel $\hat{n}(V = 0)$. In accordance with our previous findings[1] the optical and capacitive threshold voltages are identical and the shapes of $\Delta\alpha(V)/\Delta\alpha_{max}$ agree qualitatively with those of $\Delta C(V)/\Delta C_{max}$ (c.f. Figure 4, Figure 5). Graph T —which is due to the transverse transition moment of the T-dye the mirror image of the L-dye graphs—shows some voltage dependent interference pattern (Figure 5). This pattern is the result of the voltage dependence of the optical path differences in the nematic host which are not buried by the still small T-dye extinction despite the large dye concentration used. Analogously to the capacitive measurements in Figure 4 RO-TN-655 reaches 90% of the total change of extinction at $V_{90} = 4.6$ volts, i.e. 1 volt lower than

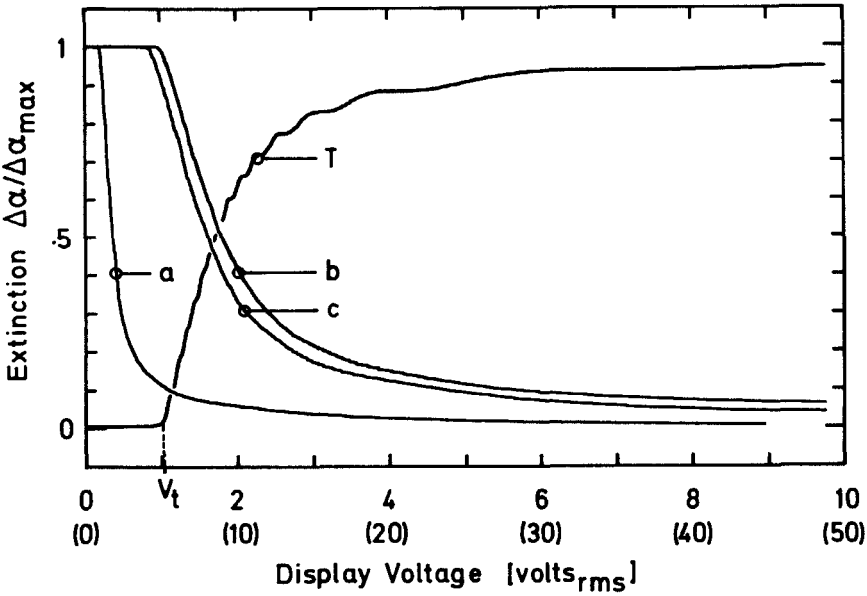


FIGURE 5 Measurements of the voltage dependence of the optical transmission of parallel aligned nematic guest-host layers containing the blue L-dye B (graphs a, b and c) and the red T-dye (graph T). Graphs b and T were recorded using RO-TN-605; for graphs a and c RO-TN-655 was used. The recordings were made at the respective extinction maxima with light polarized parallel $\hat{n}$. The voltages in brackets refer to graph a only.

RO-TN-605 (c.f. graphs *c* and *b* in Figure 5), whereas $\Delta\alpha(V)/\Delta\alpha_{max} = 1$ was reached only for voltages $V > 30$ volts (*a* in Figure 5).

Figure 6 shows the measured and calculated (dashed curves) voltage dependences $\Delta\alpha(V)/\Delta\alpha_{max}$ made with the same displays as those used for the measurements depicted in Figures 4 and 5. The indices *m* and *c* in Figure 6 refer to "measured" and "calculated" respectively. Graphs b and T were made with RO-TN-605 as a host, whereas host RO-TN-655 belongs to graph a. The numerical calculations were made using the formalism derived above together with the material parameters measured for the respective hosts (Tables I and III). Comparing the calculated with the measured characteristics in Figure 6 shows that the maximum deviation is better than 3% for the two different L-dye guest-host mixtures a and b. The deviation is larger for graphs T in which case the measured graph shows a pronounced interference pattern. This larger discrepancy is due to the five-times lower T-display extinction in which case the electro-optical properties of the host seem no longer negligible. However, the agreement shown in Figure 6 stays within the expected uncertainties of the approximations used in Section A.

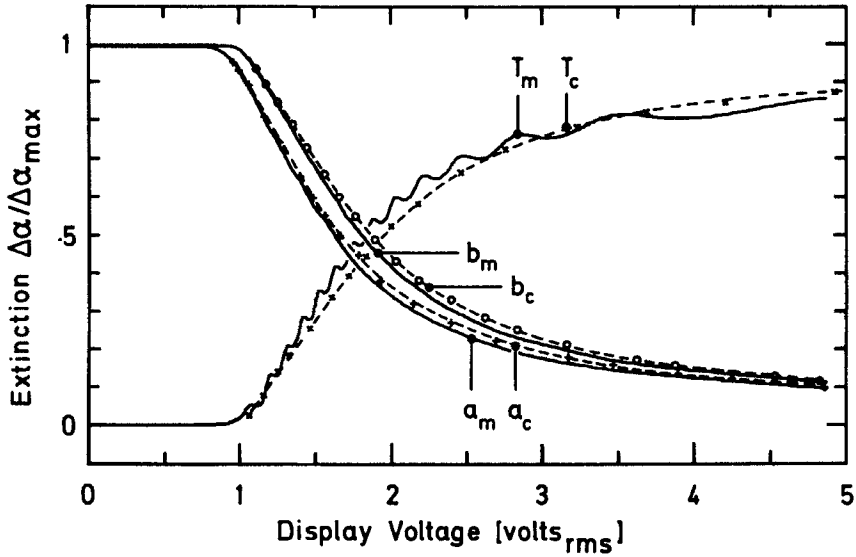


FIGURE 6 Measured (solid lines, indices m) and numerically calculated (dashed lines, indices c) optical transmission characteristics of parallel aligned nematic guest-host displays. RO-TN-605 containing dyes B and T was used as a host for the recordings b and T respectively. RO-TN-655 was the host used for graphs a.

The photograph in Figure 7 shows two homogeneously aligned nematic L/T-displays[1] containing RO-TN-605 as a host and the guest combinations $B + T$ (blue-red transition) and $Y + T$ (yellow-red transition) respectively. An impractically large T-dye concentration of 22% had to be used. The displays are operated in reflection at 4.5 volts. Because the contrast of L/T-displays is basically due to the field-induced colour change[1] such displays do not have to be operated at 100% saturation voltage (Figure 5) to achieve a good contrast (Figure 7).

## PHASE-CHANGE GUEST-HOST DISPLAYS WITH HOMOGENEOUS AND HOMEOTROPIC BOUNDARIES

Alternative guest-host displays that can be operated without polarizers are those containing optically active additives in the nematic host. The electric field-induced cholesteric nematic phase transition which reorients the dichroic guest molecules leads to the electro-optical contrast of the display.[2] The cells can be operated with homeotropic or parallel (homogeneous) wall alignment. To obtain insight into the complex field-induced realignment process of dichroic guest molecules during the phase-change

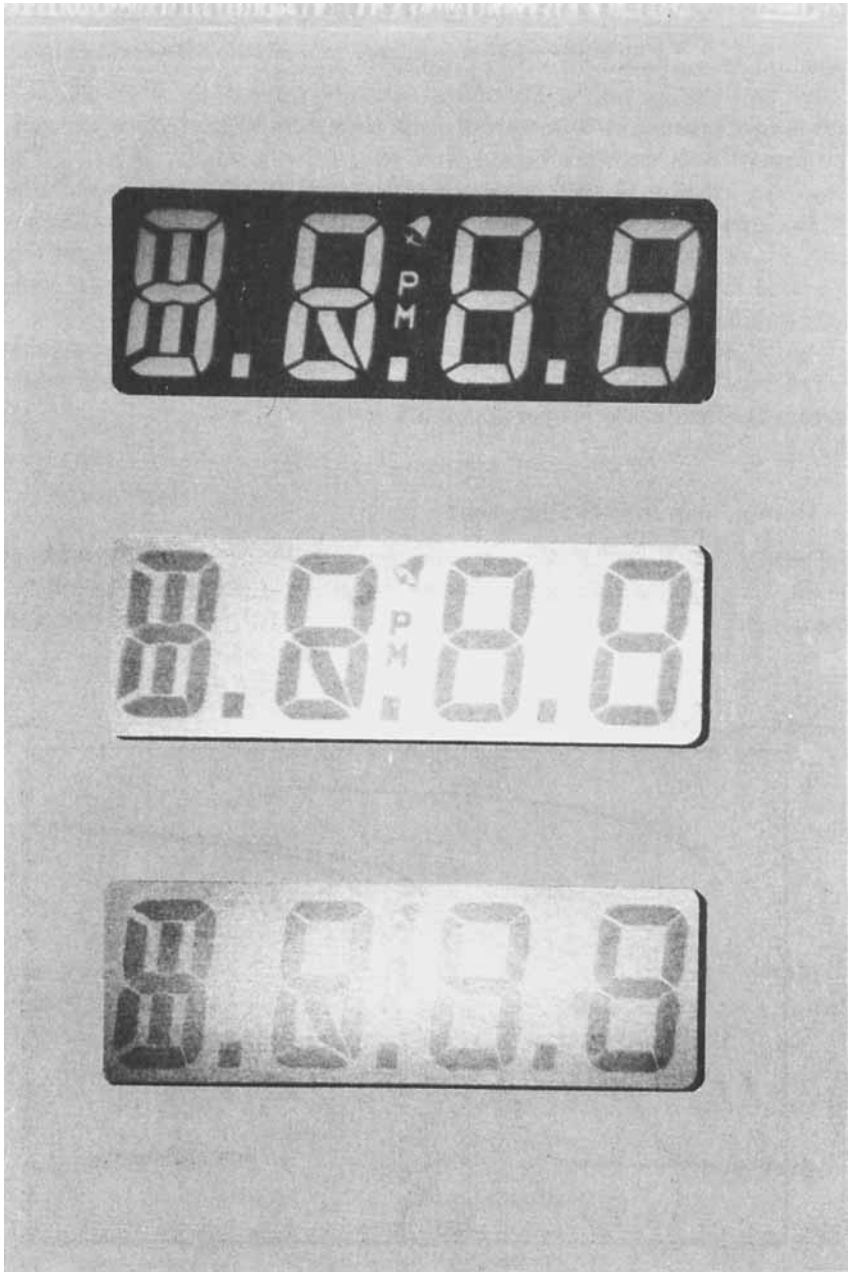


FIGURE 7 Reflective phase-change guest-host display operated at 5.5 volts containing black-white mixture G; no polarizers used (first display from the top). Reflective nematic L/T-displays with parallel wall alignment operated at 4.5 volts containing RO-TN-605 as a host (second and third display from the top). One polarizer aligned parallel to the back wall alignment was used in front of the reflector of the L/T-displays.

transition we measured the voltage dependence of the dielectric changes and related them to the voltage dependent dye absorption of the displays. Cells with homogeneous and homeotropic wall alignment were used respectively. The experiments were performed with $10 \pm 0.2$ $\mu$m display spacing. The guest-host mixture G used consisted of the host RO–TN–605 containing 3% (weight) of the optically active biphenyl CB15 from British Drug Houses and 1.5% of the black dye mixture B11 (Figure 3). A pitch $p = 4.15$ $\mu$m was measured for mixture G at 22°C. The electro-optical measurements were made in reflection using white light.

Figure 7 shows a photograph of a 7 $\mu$m phase-change guest-host display with homeotropic boundaries containing the large contrast black-white mixture G. The display is operated at 5.5 volts.

### A Homogeneous wall alignment

The recordings shown in Figure 8 are quasi stationary measurements of the field-induced capacitance changes occurring during the cholesteric-nematic phase transition in guest-host displays with homogeneous wall

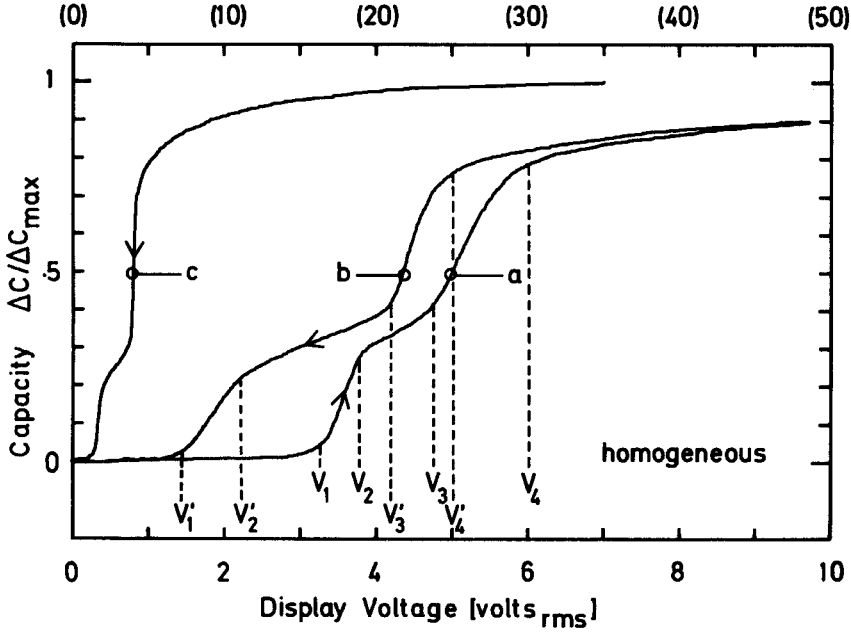


FIGURE 8 Voltage dependence of the capacitance of a parallel aligned guest-host phase-change layer. The voltages in brackets refer to measurements c only. Mixture G was used.

alignment using mixture G. The arrows indicate the sweeping direction of the cell voltage. Graph c was recorded using voltages up to 35 volts. It shows that virtually complete homeotropic alignment occurs only at voltages far above the actual cholesteric-nematic transition.

Graphs a and b in Figure 8 were recorded with a sweeping rate of 1 volt/10 minutes. Besides a pronounced hysteresis the measurements show a stepwise increase of $\Delta C(V)/\Delta C_{max}$ with increasing voltage. The steps in Figure 8 are well defined by the threshold voltages $V_1 - V_4$ and $V'_1 - V'_4$ respectively. Except for the hysteresis, graphs a and b in Figure 8 exhibit the same voltage dependence. This finding indicates that analogous intermediate phases occur for increasing and decreasing fields respectively. The threshold voltages separate five distinct regions in the phase-change transition. In the first region where $V < V_1$ (graph a in Figure 8) the measured dielectric constant of the layer was found to correspond to $\varepsilon(V < V_1) \equiv \varepsilon_\perp$ which is in agreement with the planar helical structure (Grandjean state) existing in the off-state. The pronounced capacitance increase measured in region 2 where $V_1 < V < V_2$ indicates that the Grandjean state becomes increasingly distorted in such a way that a considerable proportion of long nematic axes tend to align perpendicular to the electrode boundaries. This trend continues in a less pronounced manner in region 3, where $V_2 < V < V_3$, and becomes very pronounced again in region 4 where $V_3 < V < V_4$ (Figure 8). At the saturation voltage $V_4$ the transition from the cholesteric off-state into the homeotropic nematic on-state is essentially completed. However, voltages $V \gg V_4$ are necessary to sufficiently reduce the remaining homogeneous boundary layers at $V = V_4$ (c.f. graph c in Figure 8). Kashnow *et al.*[9] who made dielectric measurements of phase-change transitions using increasing electric fields only, reported a behaviour similar to that exhibited by graph a in Figure 8. However, their experiments did not resolve the transition regions $0 < V < V_1$, $V_1 < V < V_2$ and $V > V_4$ respectively.

Figure 9 shows reflection measurements of the voltage dependent black to white contrast change governed by the field-induced realignment of the dichroic guest dyes during the phase-change. The measurements were made with the same cell as those in Figure 8. Contrary to the dielectric measurements (Figure 8) only small electro-optical changes $<10\%$ were found for voltages $V < V_3$ and $V < V'_3$ respectively (Figure 9). The measurements show that the voltage $V_3$ is the major optical threshold. The optical changes occurring at $V_1$ and $V_2$ (Figure 9) are hardly visible to the eye. This finding is surprising considering the pronounced homeotropic aligning tendencies of the long nematic- and consequently also the dye-axes shown by the dielectric measurements in this voltage range (Figure 8). The threshold voltage $V'_2$ corresponding to $V_2$ could not be detected (c.f. graph b in Figure 9). Table IV

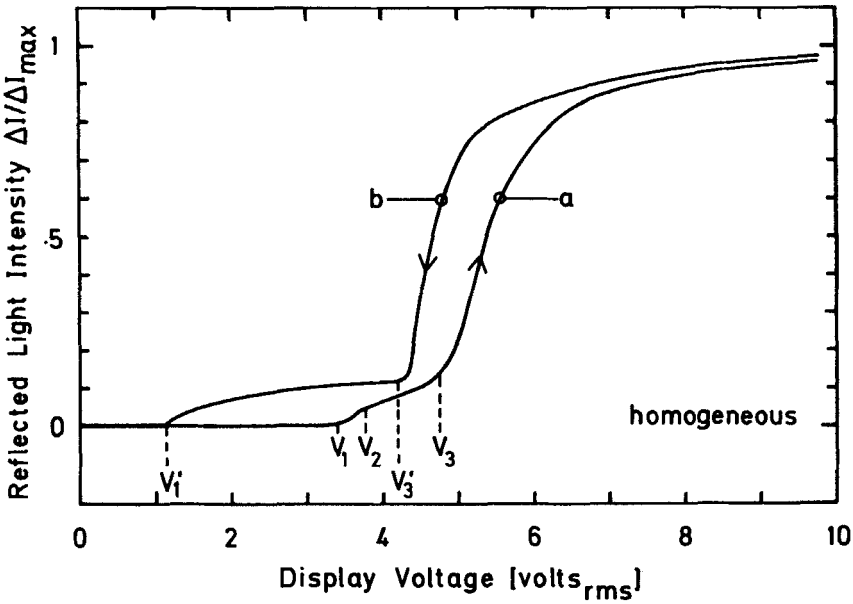


FIGURE 9 Measured voltage dependence of the (dye) extinction of a reflective guest-host phase-change display with parallel wall alignment containing the black-white mixture G.

TABLE IV

Capacitive and optical threshold voltages of homogeneously and homeotropically aligned phase-change guest-host displays respectively containing mixture G. The top two lines refer to homogeneous boundaries and the bottom two lines to homeotropic ones.

| | $V_1$; $V'_1$ (volts) | $V_2$; $V'_2$ (volts) | $V_3$; $V'_3$ (volts) | $V_4$; $V'_4$ (volts) |
|---|---|---|---|---|
| Capacitive threshold | 3.3; 1.4 | 3.8; 2.2 | 4.8; 4.2 | ~5.8; ~5.2 |
| Optical threshold | ~3.3; ~1.4 | ~3.8; — | ~4.8; 4.2 | ~6.0; ~5.0 |
| Capacitive threshold | 2.2; — | 2.8; — | 3.4; — | ~3.9; ~3.2 |
| Optical threshold | 2.4; — | 2.8; — | ~3.5; — | 4.4; ~3.4 |

shows good agreement between the dielectric and optical threshold voltages resulting from the measurements of Figures 8 and 9.

To obtain further insight into the field-induced distortion of the cholesteric phase and its influence on the optical appearance of guest-host displays we

investigated the microscopic textures of the cells in transmission with a polarizing microscope. In region 1 where $V < V_1$ (Figures 8 and 9) the eliptically polarized uniformly bright Grandjean state was observed with the axis of the right-handed planar helix aligned perpendicular to the boundaries. At voltages $V_1 \lesssim V < V_2$ a uniform fingerprint texture started to grow. Most fingerprints were aligned parallel to the direction of wall alignment. Fingerprints tending to grow in other directions were forced into meandering structures aligning parallel to the wall alignment. The top photograph in Figure 10 shows the two different fingerprint patterns developing into the uniformly bright Grandjean state. At $V = V_2$ a uniform parallel fingerprint pattern was established. The fingerprint structure indicates that the initially vertically aligned helical axis rotates in the voltage range $V_1 < V < V_2$ into a position parallel to the boundaries and perpendicular to the direction of wall alignment. This finding is in agreement with the corresponding increase of the capacity (Figure 8).

Increasing the voltage into region 3, i.e. $V_2 \lesssim V < V_3$, created an aesthetically attractive "knitting pattern." The fingerprint texture remained essentially the same as in region 2 but new instabilities occurred in some of the fingerprints leading to a substructure which is shown in the bottom photograph of Figure 10. The instabilities and the rather weak capacitance changes (Figure 8) observed in region 3 indicate that the fingerprint structure gets periodically compressed at those nodal points where the nematic directors are aligned parallel to the boundaries. In agreement with our measurements such a structural change should not lead to a strong capacitance change (Figure 8). Similar microscopic observations and interpretations of the texture in region 3 were reported by others.[9,10]

Both the fingerprint and the distorted fingerprint textures occurring in regions 2 and 3 are light scattering transition states. The propagation and polarization directions of light can therefore be assumed to be more or less randomly distributed in the cholesteric layer for voltages $V_1 < V < V_3$. Consequently the amount of light absorbed by the guest dye molecules imbedded in the fingerprint structures is much larger than one would expect from the already partially homeotropically aligned dye axis in this voltage range (Figure 8) if no scattering would occur. As a consequence the absorption of the reflective guest-host display remains virtually as low as in the off-state for voltages $V < V_3$ (Figure 9). Because scattering can only occur in optically anisotropic hosts the sharpness of the major optical threshold at $V = V_3$ and the display extinction for $V_1 < V < V_3$ are expected to depend on $\Delta n$ of the host as well as on the quality of the reflector used. Both features should degrade with decreasing $\Delta n$.

At voltages $V > V_3$ the modulated focal conic texture enters its final unwinding state leading into the homeotropic nematic phase. This transition

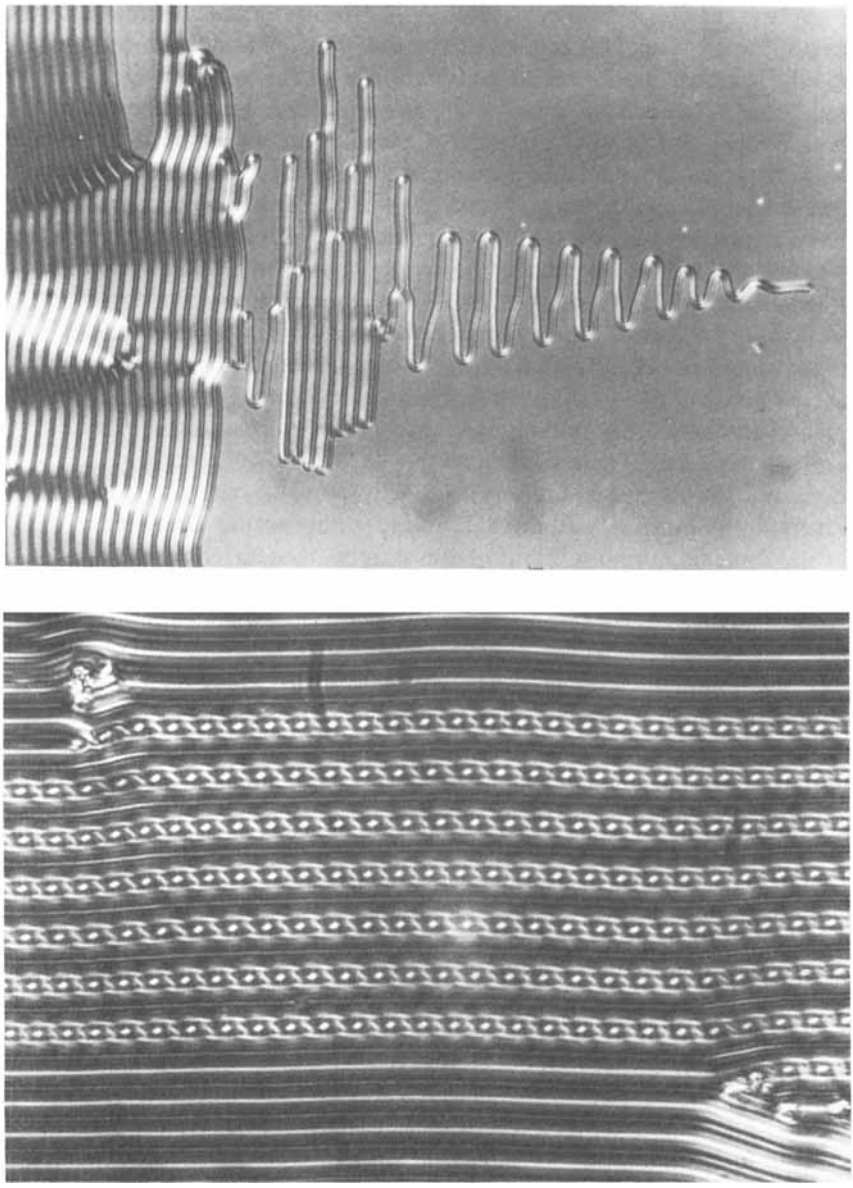

FIGURE 10 Fingerprint textures developing in the respective voltage ranges $V_1 < V < V_2$ (top photograph) and $V_2 < V < V_3$ (bottom photograph) in homogeneously aligned phase-change structures using guest-host mixture G.

is accompanied by a strong capacitance increase (Figure 8) and a decreasing density of light-scattering disinclinations. As a consequence the major optical change, i.e. switching into the white on-state occurs (Figure 9). The sluggish approach of both $\Delta C(V)/\Delta C_{max} \rightarrow 1$ and $\Delta I(V)\Delta I_{max} \rightarrow 1$ at voltages $V > V_4$ (Figures 8 and 9) is due to parallel aligned guest-host layers at the boundaries requiring rather large voltages to align homeotropically.

### B Homeotropic boundaries

Figure 11 shows the voltage dependence of the reflected light intensity of a phase-change guest-host display with homeotropic wall alignment containing mixture G. The graphs are similar to those found for cells with parallel wall alignment (Figure 9) indicating that the mechanisms governing the phase-transition may be comparable too. Comparing Figure 11 with Figure 9 shows that the threshold voltages in the homeotropic case are noticeably lower (Table IV). Furthermore, virtually the full contrast is obtained in the homeotropic case at the voltage $V = V_4$.

The measurements depicted in Figure 12 show the voltage dependence of the capacitance of homeotropically aligned cells. For increasing fields the dependence is analogous to the homogeneous case (Figure 8). However,

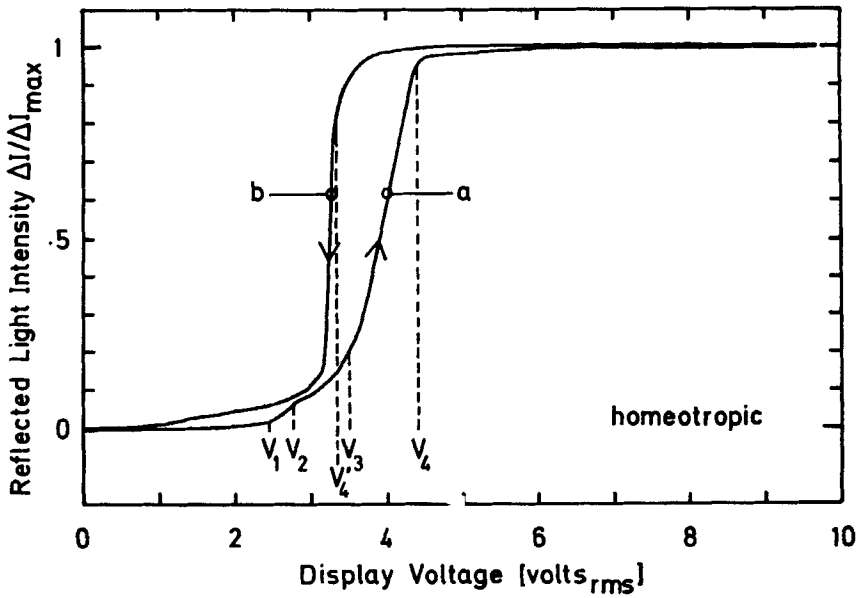


FIGURE 11 Measured voltage dependence of the (dye) extinction of a reflective guest-host phase-change display with homeotropic wall alignment containing the black-white mixture G.

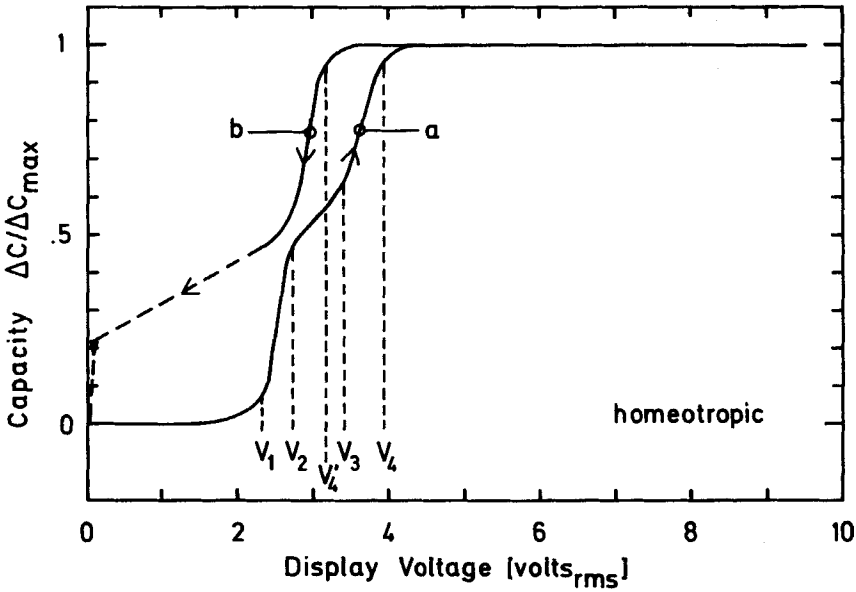


FIGURE 12 Measured voltage dependence of the capacitance of a parallel aligned guest-host phase-change layer. Mixture G was used.

$\varepsilon(V = 0)$ was found to be about 20% larger than $\varepsilon_\perp$ of the nematic host. This is due to the distorted Grandjean structure which is not perfectly planar in the off-state. In accordance with the optical measurements (Figure 11) $\Delta C(V = V_4)/\Delta C_{max} \simeq 1$ was found (Figure 12). Thus, no residual non-homeotropic boundary layers have to be realigned by large electric fields as in the homogeneous case. Our measurements indicate that many aspects of the phase transition in displays with homeotropic boundaries are similar to those in cells with parallel wall alignment. This finding is in contrast to the mechanism described by Greubel who found a focal conic-nematic transition.[11] The discrepancy between our measurements and his are likely to be due to the different measuring conditions used. Our experiments were performed very slowly thus allowing every phase to reach a quasi stationary state, whereas Greubel changed his cell voltages at a rate[11] which is likely to exclude the establishment of the stationary transition phases described here.

For decreasing fields the capacitance measurements in homeotropic cells differ from those made in homogeneous displays. After an initial steep decrease of $\Delta C(V)/\Delta C_{max}$ (graph b in Figure 12) a state with very slowly disappearing disordered fingerprint textures was reached causing the capacitance to decay extremely slowly ($\sim 10$ hours) to the stationary off-state. The

slow decay is indicated by the dashed line in Figure 12. For reasons discussed above the macroscopic extinction properties of the guest dye molecules (Figure 11) were not influenced by this slow decay. As our measuring apparatus did not allow to perform quasi stationary capacitance measurements in the dashed region of graph b in Figure 12 we could not determine whether or not the shape of the decay is analogous to graph a.

## CONCLUSIONS

We have shown how the voltage-induced changes of the capacitance of nematic and cholesteric guest-host displays are correlated with their electro-optical appearance and the material properties of liquid crystals. Transmission characteristics of parallel aligned nematic guest-host cells comprising dichroic dyes with transition moments parallel (L-dyes) and perpendicular (T-dyes) to the nematic director were investigated. Taking into account the field-induced spatial distribution of the long molecular dye axis in the display, equations were derived describing the static electro-optical behaviour for any cell voltage. Good agreement was found between measured and numerically calculated characteristics for different nematic hosts containing L and T-dyes. The new guest-host mixtures used exhibit large contrast ratios and good UV-stability. Colour-changing nematic L/T-guest-host cells as well as phase-change guest-host displays switching from a black off- to a white on-state were investigated. Measurements of the dielectric and elastic constants of pure nematic hosts and of hosts comprising dichroic dyes showed that the host properties may change noticeably when doping them with large dye concentrations (5%).

We also made measurements of the electric field-induced change of capacitance occurring in phase-change guest-host displays having homogeneous and homeotropic wall alignment respectively. The experiments show that the phase change from the cholesteric into the nematic state when using homeotropic boundaries may be more complex than suggested by Greubel.[11] Our experiments indicate that for both types of wall alignment an essentially planar helical structure exists in the off-state with the helical axis aligned perpendicular to the boundaries. At a first threshold field, which is optically hardly visible but which was found to be very pronounced in the dielectric measurements, the helical axis rotates into a position parallel to the boundaries thus giving rise to a fingerprint texture. Further increasing the field leads to a modulation of this texture and finally into the homeotropic nematic state. The major visible change of the appearance of reflective displays due to the field-induced alignment of the dye molecules in the host was shown to occur during this final transition phase. Our

measurements indicate that the sharp optical transition which is of practical importance is due to the voltage dependent scattering phenomena occurring during the phase-transition. Thus, we suspect that the sharpness depends on the optical anisotropy of the host material as well as on the mechanisms governing the phase-transition. The various transition phases occurring for increasing and decreasing field were found to be most likely identical when measured in a quasi stationary manner.

The discrepancy between the phase-transition phenomena suggested by our quasi stationary experiments and the mechanism proposed by Greubel for homeotropic boundaries and non-stationary experimental conditions can also be demonstrated by applying his equations to our measurements. The electro-optical threshold voltages denoted $V_\uparrow$ and $V_\downarrow$ by Greubel should correspond to the respective voltages $V_3$ and $V_4'$ in our measurements (Figure 11); where $V_\uparrow$ and $V_\downarrow$ are[11]

$$V_\uparrow = \pi^2 d\left(\frac{k_{22}}{\varepsilon_0 \Delta\varepsilon}\right)^{1/2} \tag{9}$$

and

$$V = \left(\frac{\pi d}{p}\right) \times \left\{\left(\frac{k_{33}}{\varepsilon_0 \Delta\varepsilon}\right) \times \left[4\left(\frac{k_{22}}{k_{33}}\right)^2 - \left(\frac{p}{d}\right)^2\right]\right\}^{1/2} \tag{10}$$

Equation (9) is identical with the threshold voltage derived by de Gennes[12] for the case when effects due to wall alignment can be neglected. From the measured material constants (Tables I, III) of RO-TN-605 and Eqs. (9) and (10) one obtains the disagreeing values $V_\uparrow = 5.8$ volts $\neq V_3 = 3.4$ volts and $V_\downarrow = 1.74$ volts $\neq V_4' = 3.2$ volts respectively. Thus, further studies will have to be made to describe the quasi stationary phase transition and its dependence on material parameters quantitatively.

Finally the dielectric and optical measurements have shown that homogeneous wall alignment in nematic as well as phase-change guest-host displays necessitates high driving voltages to achieve maximum contrast ratios. An exception are homogeneously aligned L/T-guest-host displays which—due to the colour change—do not require a perfectly homeotropic on-state.

## Acknowledgments

We wish to thank A. Boller, A. Germann and R. Marbet who synthesized the phenyldioxanes and the dichroic dyes. We also gratefully acknowledge the assistance of B. Blöchliger and J. Furler in the experimental work and wish to thank H. Krüger from Siemens Research Laboratories in Munich from whom we obtained the empty seven-segment displays used in Figure 7.

## References


1. M. Schadt, *J. Chem. Phys.*, **71**, 2336 (1979).
2. D. L. White and G. N. Taylor, *J. Appl. Phys.*, **45**, 4718 (1974).
3. G. H. Heilmeier and L. A. Zanoni, *Appl. Phys. Lett.*, **13**, 91 (1968).
4. M. Schadt and F. Müller, *IEEE Trans. Electron Devices*, **ED-25**, 1125 (1978).
5. A. Villiger, A. Boller, and M. Schadt, *Z. Nat. Forsch.*, **34b**, 1535 (1979).
6. Res. Disclosure, **189**, *Abstract Nr. 18901* (1980).
7. H. Gruler, T. J. Scheffer, and G. Meier, *Z. Nat. Forsch.*, **27a**, 966 (1972).
8. P. Gerber and M. Schadt, *Z. Nat. Forsch.*, **35a**, 1036 (1980).
9. R. A. Kashnow, J. E. Bigelow, H. S. Cole, and C. R. Stein, *Liquid Crystals and Ordered Fluids*, eds. J. F. Johnson and R. S. Porter, **2**, 483 (Plenum Press, New York, 1974).
10. M. Kawachi and O. Kogure, *Jap. J. Appl. Phys.*, **16**, 1673 (1977).
11. W. Greubel, *Appl. Phys. Lett.*, **25**, 5 (1974).
12. P. G. de Gennes, *Solid State Comm.*, **6**, 163 (1968).